Spectroscopic Studies on the Interaction of Aristololactam-β-D-Glucoside with DNA and RNA Double and Triple Helices: A Comparative Study†

A. Ray, G. Suresh Kumar, S. Das, and M. Maiti*

Biophysical Chemistry Laboratory, Indian Institute of Chemical Biology, 4 Raja S.C. Mullick Road, Calcutta 700032, India

Received September 2, 1998; Revised Manuscript Received December 3, 1998

ABSTRACT: The interaction of aristololactam-β-D-glucoside (ADG), a DNA intercalating alkaloid, with the DNA triplexes, poly(dT)·poly(dA)×poly(dT) and poly(dC)·poly(dG)×poly(dC^+), and the RNA triplex poly(rU)·poly(rA)×poly(rU) was investigated by circular dichroic, UV melting profile, spectrophotometric, and spectrofluorimetric techniques. Comparative interaction with the corresponding Watson−Crick duplexes has also been examined under identical experimental conditions. Triplex formation has been confirmed from biphasic thermal melting profiles and analysis of temperature-dependent circular dichroic measurements. The binding of ADG to triplexes and duplexes is characterized by the typical hypochromic and bathochromic effects in the absorption spectrum, quenching of steady-state fluorescence intensity, a decrease in fluorescence quantum yield, an increase or decrease of thermal melting temperatures, and perturbation in the circular dichroic spectrum. Scatchard analysis indicates that ADG binds both to the triplexes and the duplexes in a noncooperative manner. Binding parameters obtained from spectrophotometric measurements are best fit by the neighbor exclusion model. The binding affinity of ADG to the DNA triplexes is substantially stronger than to the RNA triplex. Thermal melting study further indicates that ADG stabilizes the Hoogsteen base-paired third strand of the DNA triplexes whereas it destabilizes the same strand of RNA triplex but stabilizes its Watson−Crick strands. Comparative data reveal that ADG exhibits a stronger binding to the triple helical structures than to the respective double helical structures.

The formation of RNA[1] triple helix was first described over 40 years ago (*1*). Subsequently it was established that both ribo and deoxyribopyrimidine polymers can associate with complementary double helical homopurine−homopyrimidine strands to form triple helices (*2, 3*). The formation of triple helices is an important means of achieving sequence-specific recognition of duplex DNA and RNA by oligonucleotides. The sequence specificity is primarily achieved through the formation of specific Hoogsteen type hydrogen bonds involving thymine (T) recognizing adenine−thymine (A·T) base pairs and N3-protonated cytosine (C^+) recognizing the guanine−cytosine (G·C) base pairs in DNAs and uracil (U) recognizing the adenine−uracil (A·U) base pairs in RNA (*4*−*6*). Other triplexes have also been described for recognition of T·A and G·C base pairs including A·T×G and G·C×T in parallel motif which are less stable (*7*). In recent years increasing interest has been focused on triple helical nucleic acids due to their potential biological relevance as well as their importance in therapeutic, diagnostic, and biotechnological applications (*2, 3, 8*−*13*), and extensive studies are going on with model oligonuclotides on the various aspects of triplex structures (*14*−*16*). Although the third-strand oligonucleotides possess exquisite sequence recognition properties, their binding is not so strong which results in relatively low stability of the triplex structure. One means of increasing the triplex stability is through the use of triplex-specific ligands, which bind to triplex but not to duplex DNA. Several such compounds have now been described. Ethidium (*17, 18*), acridines (*19*), coralyne (*20, 21*), anthroquinones (*22*), naphthoquinolines (*23, 24*), benzo[ϵ]pyridoindole, quinoxaline derivatives (*10, 25*), and [ruthenium (II) (1,10-phenanthridine)$_2$L]$^{2+}$ (*12*) are reported to intercalate between the nucleobases of DNA triplexes thereby stabilizing the Hoogsteen base-paired third-strand binding (*25*). Most of these molecules preferentially stabilize the T·A×T based triplexes while few compounds such as coralyne have been shown to stabilize both T·A×T and C·G×C^+ triplexes. Several biophysical studies and properties of RNA triplexes including hybrids have been reported (*26*−*28*). However, studies on ligand interaction with RNA triplexes are still scanty. Formation of poly(rU)·poly(rA)×poly(rU) triplex and its interaction with ethidium were reported first by Waring (*29*) and subsequently by Lehrman and Crothers (*30*). Later results showed that ethidium destabilizes this RNA triplex, and the drug was shown to have lower affinity for the triplex when compared with the duplex (*18*). More recently, Breslauer and co-workers (*31*) have reported the binding of berenil to poly(rU)·poly(rA)×poly(rU) triplex. Thus, the strategy of stabilizing the DNA and RNA triplexes

† This research was partially supported by a grant (SP/SO/D-21/91) from the Department of Science & Technology, Government of India, to M.M.

* To whom all correspondence should be addressed. E-mail: IICHBIO@GIASCL01.VSNL.NET.IN. Fax: 0091-33-473-0284/5197.

[1] Abbreviations: ADG, aristololactam-β-D-glucoside; DNA, deoxyribonucleic acid; RNA, ribonucleic acid; ·, Watson−Crick base pairing between the homopyrimidine strand I and the homopurine strand II; ×, Hoogsteen base pairing between homopurine strand II and the homopyrimidine strand III; DMSO, dimethyl sulfoxide; CD, circular dichroism; EDTA, ethylenediaminetetraacetic acid; T_m, thermal melting temperature; P/D, nucleotide phosphate (duplex/triplex)/drug molar ratio; D/P, drug/nucleotide phosphate (duplex/triplex) molar ratio.

10.1021/bi982128n CCC: $18.00
Published on Web 04/24/1999

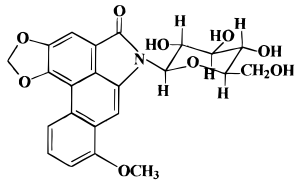

FIGURE 1: Chemical structure of aristololactam-β-D-glucoside.

under physiological conditions by specific interaction with ligands is of considerable current significance.

Aristololactam-β-D-glucoside (ADG) or 6-β-D-glucopyranosyl-8-methoxy-benzo[*f*]-1,3-benzodioxolo[6,5,4-*cd*] indol-5(6*H*)-one (Figure 1) belongs to the aristolochia group of plant alkaloids that have attracted recent attention for their prospective clinical and pharmacological uses (*32*, *33*). This phenanthrenic lactam derivative is of significant interest for its attached glucoside ring. ADG shows remarkable structural stability in a wide range of pH, with a p*K* value of 12.7 (*34*). Recently, it has been shown that the alkaloid binds strongly to B-form duplex DNA by the mechanism of intercalation with considerable sequence specificity toward GC-rich DNA, especially alternating GC polymer (*35*−*38*) while it does not bind to left-handed Z-DNA (*39*). ADG also inhibits both the rate and extent of the B to Z transition and converts Z-DNA to the bound B-form structure (*39*).

In the present study we have sought to characterize the capability of ADG to stabilize nucleic acid triplex structures. Toward this, we have investigated the interaction of ADG with two DNA triplexes, poly(dT)·poly(dA)×poly(dT) and poly(dC)·poly(dG)×poly(dC^+), and the RNA triplex, poly(rU)·polyl(rA)×poly(rU), using various spectroscopic techniques. Our study also examines under identical solution conditions the interaction of this alkaloid to the parent double helical polymers for a meaningful comparison of the data. The results provide evidence for a strong DNA triplex stabilizing capability of this alkaloid. Further, this report also presents the first spectroscopic evidence, to date, of binding of a DNA binding intercalator, other than ethidium to the RNA triplex poly(rU)·poly(rA)×poly(rU).

EXPERIMENTAL PROCEDURES

Poly(dT), poly(dA)·poly(dT), poly(dC), poly(dG)·poly(dC), poly(rU), poly(rA)·poly(rU), and poly(rU)·poly(rA)×poly(rU) were obtained from Sigma Chemicals Co., St. Louis, MO. These compounds were of the highest grade commercially available and were always tested for their nativeness and purity by UV absorption, T_m, and CD characteristics (*38*−*40*). Each polymer concentration was determined spectrophotometrically at the indicated wavelengths (nm) using the following molar extinction coefficients, ϵ (M^{-1} cm^{-1}), expressed in terms of nucleotide phosphates: ϵ_{265} of poly(dT) = 8700, ϵ_{260} of poly(dA)·poly(dT) = 6000, ϵ_{260} of poly(dC) = 7400, ϵ_{253} of poly(dG)·poly(dC) = 7400, ϵ_{260} of poly(rU) = 9350, ϵ_{260} of poly(rA)·poly(rU) = 7140, ϵ_{257} of poly(rU)·poly(rA)×poly(rU) = 5900. ADG was extracted from *Aristolochia indica* and was crystallized from ethanol. Its purity was checked by thin-layer chromatography and melting point determination, and further characterization was done by UV−vis, fluorescence, and mass and NMR spectral analysis as described earlier (*34*, *35*). The concentration of ADG was obtained spectrophotometrically using the molar extinction coefficient (ϵ) 10930 M^{-1} cm^{-1} (λ_{398}) in DMSO (*37*, *38*). Polynucleotide stock solutions were prepared in BPES buffer (20 mM [Na^+]), pH 7.0, containing 1.5 mM Na_2HPO_4, 0.5 mM NaH_2PO_4, 0.25 mM Na_2EDTA, and 16 mM NaCl. Studies on triple and double helical DNAs were carried out in 10 mM sodium cacodylate−HCl buffer containing 300 mM NaCl, 0.1 mM Na_2EDTA, and 240 mM DMSO at pH 6.8 (310 mM [Na^+]) (designated as SCH buffer I), or in 10 mM sodium cacodylate−HCl buffer containing 100 mM NaCl, 0.1 mM Na_2EDTA, and 240 mM DMSO at pH 5.5 (110 mM [Na^+]) (designated as SCH buffer II). Studies on triple helical RNA were carried out using 10 mM sodium cacodylate−HCl buffer containing 25 mM NaCl, 0.1 mM Na_2EDTA, and 240 mM DMSO at pH 6.9 (35 mM [Na^+]) (designated as SCH buffer III). Glass-distilled deionized water and analytical grade reagents were used throughout. pH measurements were made on an Electronic Corporation (India) pH meter with an accuracy of ±0.01 units.

Formation of Triple Helical Structures. Poly(dT)·poly(dA)×poly(dT) (hereafter T·A×T) ("dot" and "cross" represents Watson−Crick and Hoogsteen base pairing, respectively) triple helix was prepared by mixing the two polynucleotide solutions, poly(dT) and poly(dA)·poly(dT) (hereafter A·T), in 1:1 molar ratio in 10 mM sodium cacodylate buffer containing 300 mM NaCl (pH 6.8) at 15 °C (*41*). Solutions were heated to 90 °C and cooled slowly at a rate of 0.5 °C/min to 5−10 °C. Poly(dC)·poly(dG)×poly(dC^+) (hereafter C·G×C^+) triple helix was prepared by mixing equimolar amounts of poly(dC) and poly(dG)·poly(dC) (hereafter G·C) stock solutions at 10 °C (*42*) under constant stirring for 1−2 h in 10 mM sodium cacodylate buffer containing 100 mM NaCl (pH 5.5). To a cold solution of the buffer was first added poly(dG)·poly(dC), and the mixture was allowed to stand for 10−15 min to attain equilibrium. Thereafter, the appropriate amount of poly(dC) was added. Poly(rU)·poly(rA)×poly(rU) (hereafter U·A×U) triple helix was prepared either by dissolving the RNA triplex (Sigma sample) in 10 mM sodium cacodylate buffer containing 25 mM NaCl (pH 6.9) (*43*) or by mixing poly(rU) and poly(rA)·poly(rU) (hereafter A·U) in 1:1 molar ratio in the same buffer, heating to 90 °C, and then cooling to 15 °C (*41*, *43*). Formation of each triplex was confirmed by its characteristic CD spectrum (*44*, *45*) and melting profile (*41*, *46*).

Thermal Melting Study. Absorbance versus temperature profiles for nucleic acids and their complexes with alkaloid in appropriate solution conditions were measured at particular wavelengths using a Shimadzu UV-260 spectrophotometer (Shimadzu Corporation, Kyoto, Japan) equipped with a thermoelectric cell temperature controller (SPR-5) and temperature programmer (KPC-5) in Teflon-capped quartz cuvettes of 1 cm path length. The temperature was scanned using a heating rate of either 0.5 or 1.0 °C per minute. The melting profile was obtained either as a direct plot or as data points which were later manually plotted. T_m was obtained from the derivative plot, and the manual plot gave identical values.

Circular Dichroism. CD measurements were carried out on a JASCO J720 spectropolarimeter (Japan Spectroscopic Ltd., Japan) attached with a temperature controller and

thermal programmer model PTC 343 interfaced with a COMPAQ PC 486 in rectangular quartz cuvettes of 1 cm path length as reported earlier (*38, 39*). Each spectrum was averaged from five successive accumulations and was baseline-corrected and smoothed using the software supplied by JASCO.

UV−Visible Spectroscopy. The UV−visible absorption spectra of ADG mixed with or without duplex or triplex were obtained using the Shimadzu UV-260 spectrophotometer (Shimadzu Corp., Kyoto, Japan) in a thermostatically controlled cell holder equipped with a thermoprogrammer (KPC-5) and a temperature controller (SPR 5) in matched quartz cells of 1 cm path length generally following the methods described earlier (*39*). The decrease in absorbance of the alkaloid at 398 nm upon binding to duplex or triplex was used to calculate the equilibrium concentration of free and bound alkaloid. In all the mixtures, alkaloid concentration was kept constant and changes in the P/D were effected by the gradual addition of increasing concentration of duplex or triplex. The correction factor due to dilution was also applied wherever necessary. The rate of formation of the complex appeared to be very rapid. Readings obtained a few seconds after mixing remained unchanged even after a long lapse of time (1−2 h). In practice, solutions were allowed to stand for at least 5 min at the specific temperature before the readings were taken. Binding studies with DNA triplexes T·A×T and C·G×C$^+$ were carried out at 15 °C and 10 °C, respectively, while that with the RNA triplex U·A×U was carried out 15 °C. All the spectroscopic studies below 15 °C were done with constant purging of nitrogen gas to prevent moisture condensation on the optical windows.

Data Analysis. Binding data obtained from spectrophotometric titration were cast into the form of the Scatchard plot of r/C_f versus r, where r is the number of alkaloid molecules bound per mole of nucleotide (duplex/triplex) and C_f is the molar concentration of the free alkaloid. Nonlinear binding isotherms were observed in each case, and the data were fitted to a theoretical curve drawn according to the excluded site model (*47*) developed by McGhee and von Hippel (*48*) for a nonlinear noncooperative ligand binding system using the following equation

$$r/C_f = K'(1 - nr)[(1 - nr)/(1 - (n - 1)r]^{(n-1)} \quad (1)$$

where K' is the intrinsic binding constant to an isolated binding site and n is the number of nucleotides occluded by the binding of a single ligand molecule. Binding data were analyzed using the program SCATPLOT version 1.2 (*49*) which works on an algorithm (*50*) that determines best fit parameters to eq 1. The binding parameters r and C_f are determined from the change in absorbance at a particular wavelength (usually, the absorption maximum of the free alkaloid) as described earlier (*39, 40*).

Spectrofluorimetric Studies. Steady-state fluorescence measurements were performed on a Hitachi F-4010 spectrofluorimeter (Hitachi Ltd., Tokyo, Japan) to which was attached an EYELA UNICOOL UC-55 (Tokyo Rikakikai Co. Ltd., Tokyo, Japan) temperature controller. Measurements were made in fluorescence-free quartz cells of 1 cm path length as described earlier (*40*). Uncorrected fluorescence spectra are recorded. The steady-state fluorescence quantum yield was calculated as described by Ray and Maiti (*39*).

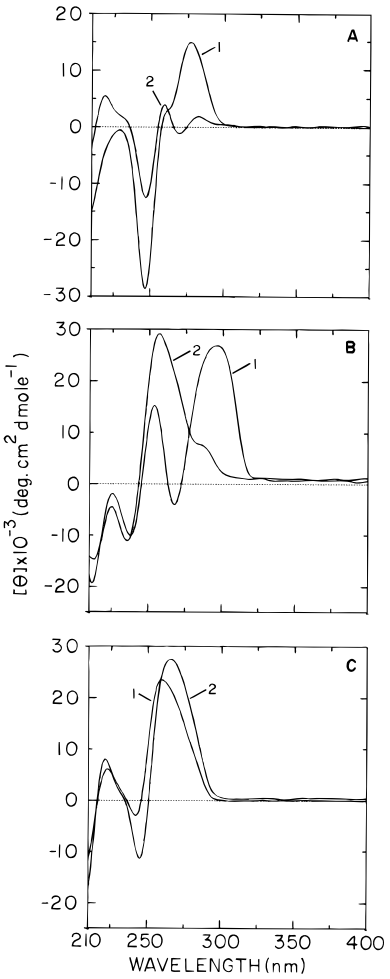

FIGURE 2: Circular dichroic spectra of triplex and duplex structures: (A) T·A×T triplex (60.82 μM, curve 1), A·T duplex (70 μM, curve 2); (B) C·G×C$^+$ triplex (39.52 μM, curve 1), G·C duplex (60.54 μM, curve 2); and (C) U·A×U triplex (70.76 μM, curve 1), A·U duplex (74.11 μM, curve 2).

RESULTS

Characteristics of Triple Helical Structures. The formation of the two DNA triplexes T·A×T and C·G×C$^+$ and the RNA triplex U·A×U was confirmed from CD and thermal melting studies. The CD spectra of these triplexes and the corresponding duplexes are shown in Figure 2. In Figure 2A, the T·A×T spectrum (curve 1) is characterized by a positive band in the 275−280 nm region followed by a large negative band around 248 nm. A shoulder in the 260−265 nm region with positive ellipticity is yet another characteristic in the CD of this triplex. The CD characteristics of this triplex are remarkably different from those of the A·T duplex (curve 2) which has two small positive bands in the 260−280 nm region, followed by a negative band at 250 nm, and a positive band in the 210 nm region. Figure 2B depicts the characteristic CD spectrum (curve 1) of the C·G×C$^+$ triplex along with that of the G·C duplex. The triplex CD is characterized by the presence of two positive bands, one in the 250−260 nm and another in the 290−300 nm region, and two negative bands, a weak one in the 265−270 nm region and a relatively strong band in the 230−240 nm region, whereas the duplex

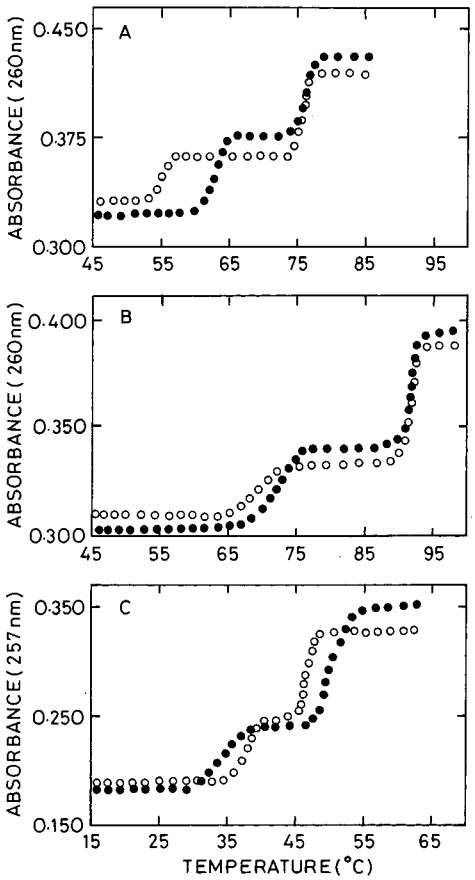

FIGURE 3: Thermal melting profiles of DNA and RNA triplexes and their complexation with ADG: (A) 19.98 μM of T·A×T triplex (○-○) and its complex with ADG (●-●) at D/P 0.40 in SCH buffer I; (B) 30.02 μM of C·G×C$^+$ triplex (○-○) and its complex with ADG (●-●) at D/P 0.38 in SCH buffer II; and (C) 31.77 μM of U·A×U triplex (○-○) and its complex with ADG (●-●) at D/P 0.39 in SCH buffer III.

has a large positive CD near 260 nm. Here, again, there are large differences in both the nature and intensity of bands between the triplex and the duplex spectrum. In Figure 2C, the CD spectrum of the RNA triplex, U·A×U (curve 1), and that of the duplex, A·U (curve 2), are depicted. The triplex is characterized by a positive band at 260 nm and a negative band in the 243 nm region, and both these bands have lower ellipticity values compared to that of the duplex.

The melting profiles characterizing these triplexes show biphasic transitions (Figure 3A,B); the first transition represents the displacement of the third strand from the triplex while the second transition represents the duplex denaturation to single strands. It was observed that the melting profile of each polymer was identical for a heating rate of either 1.0 or 0.5 °C/min, indicating that enough time was allowed for thermal equilibrium. In case of the T·A×T and C·G×C$^+$ triplexes, the first T_m was at 55 and 69 °C, followed by the second T_m at 76 and 92 °C, respectively. The RNA triplex U·A×U also showed a biphasic melting pattern (Figure 3C) with T_ms at 37 and 46.5 °C, respectively, the second transition representing the duplex denaturation. The biphasic melting of all these triplexes with the second transition temperature corresponding to that observed with their parent duplexes clearly indicated the formation and stability of these triplexes. Similarly, temperature-dependent CD spectral measurements (not shown) of these triplexes were performed. It was

Table 1: Effect of ADG on the Thermal Stability of Triplex DNA and RNA[a]

polymer/ complex	D/P	[Na$^+$] (mM)	T_m' (°C) 3→2	T_m'' (°C) 2→1	$\Delta T_m'$ (°C) 3→2	$\Delta T_m''$ (°C) 2→1
T·A×T	0	310	55.0	76.0		
T·A×T+ADG	0.40	310	62.0	76.0	7.0	0.0
C·G×C$^+$	0	110	69.0	92.0		
C·G×C$^+$+ADG	0.38	110	72.5	91.5	3.5	−0.5
U·A×U	0	35	37.0	46.5		
U·A×U+ADG	0.39	35	34.5	50.0	−2.5	3.5

[a] Average from three experiments for each triplex. Error limits for individual measurements are estimated at ±0.5 °C in T_m. T_m'(3→2) and T_m''(2→1) are triplex to duplex and duplex to single-strand transition, respectively. ΔT_m = [T_m of complex − T_m of triplex DNA or RNA].

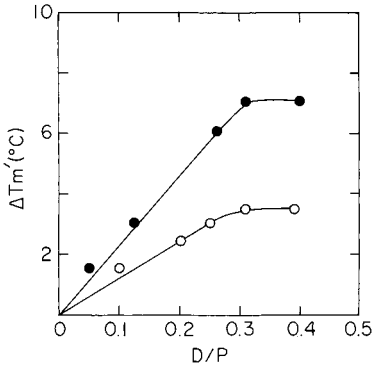

FIGURE 4: A plot of $\Delta T_m'$ versus different D/P molar ratios. Key: T·A×T triplex (●-●) and C·G×C$^+$ triplex (○-○).

observed that the conformational changes indicated an initial displacement of the third strand followed by duplex denaturation at temperatures corresponding to that observed in UV melting experiments.

Thermal Melting Studies of ADG−Duplex and Triple Helical Structures. To examine the effect of the alkaloid on the stability of these triple helices, we have studied the thermal denaturation of each triplex in the presence and absence of ADG. Figure 3 illustrates the effect of ADG on the thermal stability of the three triplexes. The results show that ADG stabilized both T·A×T (Figure 3A) and C·G×C$^+$ (Figure 3B) triplexes in that their triplex to duplex transition temperature was enhanced by 7 and 3.5 °C, respectively, at saturation (Table 1). There was no effect of ADG whatsoever on the duplex denaturation temperature as no change in the T_m was observed on the second thermal transition. The results further show that the T_m of the first melting transition increases with increasing concentration of ADG. Figure 4 shows the increase in T_m of the first melting for the third strand ($\Delta T_m'$) with D/P ratio.

The thermal transition profiles of the corresponding double helices complexed with ADG (not shown) showed biphasic transitions, one at the higher temperature side identical to that obtained for the free double stranded form and another at a lower temperature side. The T_m values appeared at 65 and 76.2 °C for the A·T duplex while for the G·C duplex it was observed at 74 and 93.5 °C, respectively (Table 2). The presence of a lower temperature transition can be interpreted in terms of a binding mode that induces destabilization to both duplex structures at high salt molarity. The ligand-induced destabilization in the case of the G·C duplex can be rationalized due to the conformational status of the DNA

Table 2: Effect of ADG on the Thermal Stability of Duplex DNA or RNA[a]

polymer	D/P	[Na^+] (mM)	T_{m_l} (°C)	T_{m_h} (°C)	ΔT_m[b] (°C)
A·T	0	310		76.0	
A·T + ADG	0.41	310	65.0	76.2	0.2
G·C	0	110		93.1	
G·C + ADG	0.39	110	74.0	93.5	0.4
A·U	0	35		45.5	
A·U + ADG	0.40	35		49.0	3.5

[a] Average from three experiments for each duplex. T_{m_l} and T_{m_h} represent the lower and higher temperature side. Error limits for individual measurement in T_m are estimated to be ±0.5 °C. [b] ΔT_m = [T_m of complex − T_m of duplex DNA or RNA].

structure at high salt molarity which is different from the canonical B-form structure as pointed out by Quali et al. (*42*) and Tuite et al. (*51*). At low molarity the A·T duplex is not in a regular B-form structure (*52*), but at 310 mM [Na^+] it has adopted a certain conformational modification and this duplex structure exhibits two thermal melting profiles on binding to ADG. In this context, it is interesting to note that at low ionic strength (20 mM [Na^+]) ADG does not bind to the A·T duplex as demonstrated by Nandi et al. (*38*).

Figure 3C displays the thermal transition profile of U·A×U triplex in the presence of ADG. The melting profile of the complex showed destabilization of the triplex by the alkaloid ($\Delta T_m = -2.5$ °C) at that D/P ratio of 0.39. On the other hand, the characteristic duplex to single-strand transition was stabilized by the alkaloid. A similar result was obtained by Waring (*29*) with ethidium and by Breslauer and co-workers (*41*) for berenil. The A·U duplex−ADG complex showed a higher melting temperature compared to the free polymer as expected (Table 2). The quantitative data of the melting temperature of these three triplexes and the corresponding duplexes and that of their ADG complexes are compared in Tables 1 and 2. Taken together, it can be generalized that ADG stabilizes the triplex structures of DNA while it destabilizes the RNA triplex.

CD Study of ADG Interaction with Double and Triple Helical Structures. Further evidence for the interaction of the alkaloid with various duplex and triplex structures of DNA and RNA was obtained from the CD spectral measurements in the 240−450 nm region. In the presence of ADG, the A·T duplex and T·A×T triplex (Figures S1A and S1B, Supporting Information), the G·C duplex and C·G×C^+ triplex (Figures S1C and S1D, Supporting Information), and the A·U duplex and U·A×U triplex (Figures S1E and S1F, Supporting Information) were perturbed. The perturbation was greater with triplex structures than with the corresponding duplex structures. In addition, an extrinsic CD band in the 350−450 nm region was observed in all triplex spectra, while no observable extrinsic CD band appeared in duplex structure spectra except in that of the AT duplex.

Absorption Spectral Studies of ADG−Duplex and −Triplex Binding. The absorption spectrum of ADG in the 300−500 nm range has two absorption maxima centered around 330 and 398 nm (Figure 5). Progressive addition of increasing concentrations of all the three triplexes effected hypochromic and bathochromic changes with the appearance of a sharp isosbestic point at 420 nm, which indicated the existence of equilibrium between free and triplex-bound forms of alkaloid.

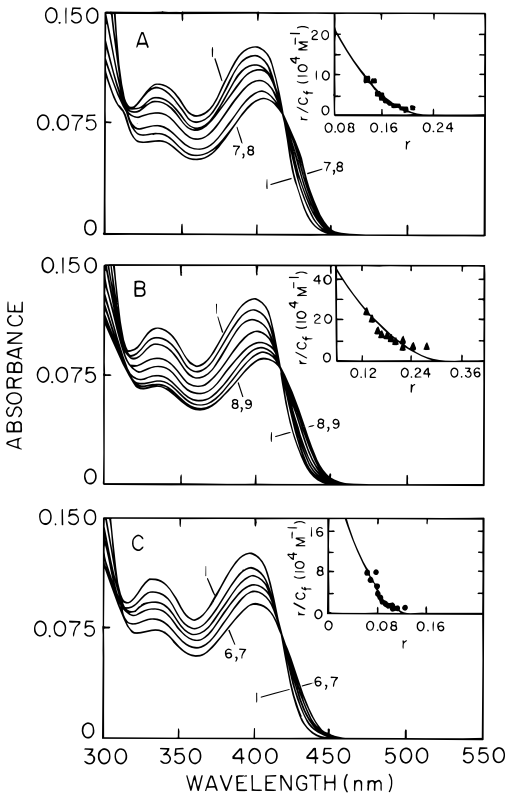

FIGURE 5: Effect of DNA and RNA triplexes on the absorption spectrum of ADG. (A) Curves 1−8 denote the absorption spectrum of ADG (12.83 μM) treated with 0, 8.64, 17.22, 34.18, 50.87, 67.30, 83.48, and 99.41 μM of T·A×T triplex, respectively, in SCH buffer I at 15 °C. (B) Curves 1−9 denote the absorption spectrum of ADG (12.42 μM) treated with 0, 6.40, 12.42, 24.52, 45.50, 56.46, 71.92, 99.36, and 113.0 μM of C·G×C^+ triplex, respectively, in SCH buffer II at 10 °C. (C) Curves 1−7 denote the absorption spectrum of ADG (12.59 μM) treated with 0, 18.53, 35.74, 63.83, 91.49, 145.51, and 171.91 μM of U·A×U triplex, respectivley, in SCH buffer at 15 °C. Inset: representative Scatchard plots for binding of ADG to (A) T·A×T triplex; (B) C·G×C^+ triplex; and (C) U·A×U triplex. The solid lines are the nonlinear least-squares best fit of the experimental points to the neighbor exclusion model (eq 1) obtained using the computer program SCATPLOT (*48*). This model adequately fits the data within the regions of the Scatchard plot ranging from 30% (lower limit) and 95% (upper limit). Values of K' and n are presented in Table 3.

The effect of the corresponding duplexes on the absorption spectrum of ADG under identical conditions of buffer was also studied (not shown). ADG showed considerable affinity toward A·T and G·C duplexes as revealed from absorption titration data. The kind of interaction with A·T duplex that is observed here, however, was absent in low salt buffers viz. 20 mM BPES as demonstrated earlier (*38*). In case of the duplex RNA, an additional isosbestic point appeared in the lower wavelength region (near 310 nm) though one was not discernible in triplex titrations, presumably characteristics of double helical A-form RNA−ADG interaction.

Evaluation of Binding Parameters. The binding constants and the number of excluded sites for the interaction of ADG with these three triplexes and the corresponding duplexes under identical solution conditions were estimated from Scatchard plots of r/C_f versus r derived from spectrophotometric titration data. The Scatchard plots in case of the triplexes are presented in the inset of Figure 5. Binding isotherms for all the triplexes (Figure 5) and the duplexes (not shown) are nonlinear and concave upward, indicating a

Table 3: Binding Parameters for ADG Complexation with Triplexes and with Corresponding Duplexes Obtained for Spectrophotometric Studies[a]

polymer	[Na^+] (mM)	K' ($\times 10^4$ M^{-1})	n (pd or pt/ ligand bound)[b]
A·T[c]	20	0	0
A·T	310	9.90 ± 0.4	11.11 ± 0.5
T·A×T	310	44.0 ± 4.0	4.44 ± 0.2
G·C[c]	20	13.0 ± 1.0	6.0 ± 0.14
G·C	110	37.0 ± 3.0	3.85 ± 0.4
C·G×C^+	110	59.0 ± 4.0	3.13 ± 0.1
A·U	35	6.85 ± 0.3	8.33 ± 0.3
U·A×U	35	25.0 ± 2.0	7.50 ± 0.2

[a] Five determinations each. [b] "pd" and "pt" are the number of phosphate nucleotides for duplex and triplex, respectively. [c] Data from Nandi et al. (*38*) are incorporated here for comparison.

negatively cooperative binding process. The quantitative binding parameters of ADG to the triple helices and their duplex counterparts derived from these plots (vide supra) are collated in Table 3. The binding constant values are remarkably higher for the triplex−ADG interaction and are about 3−4 times higher than that for duplex−ADG interaction. It is also apparent from Table 3 that the value of the intrinsic binding constant is less for the RNA triplex compared to the DNA triplexes despite the 3-fold higher salt molarity difference. For the three triple helical structures studied, the binding constant varies in the order of C·G×C^+ > T·A×T > U·A×U. The binding constant for A·T duplex−ADG complexation is $\sim 9.9 \times 10^5$ M^{-1}. This is especially noteworthy and indicates that under the present experimental conditions (310 mM [Na^+]) ADG has certainly good affinity toward this duplex structure in contrast to its rather lack of affinity observed at low ionic strength (*38*).

Fluorescence Study of ADG−Duplex and −Triplex Binding. The characteristic steady-state emission spectrum of ADG in the region of 420−620 nm has a maximum at 490 nm when excited at 400 nm. The steady-state fluorescence intensity of ADG was progressively quenched in the presence of all the triplexes and duplexes with increasing P/D ratio. Representative quenching patterns in the case of the G·C duplex and the C·G×C^+ triplex are shown in Figure S2 (Supporting Information). The quantitative data on fluorescence quantum yield (Figure S3, Supporting Information) of various ADG−triplex or ADG−duplex complexes show that the relative quantum yield decreases with increasing P/D ratio and levels off at saturation. It was observed that the interaction of ADG with the C·G×C^+ triplex and G·C duplex was strongest among the three triplexes and their corresponding duplexes. It is interesting to note that the fluorescence intensity of ADG was quenched on addition of the A·T duplex in the present experimental conditions of 310 mM [Na^+], unlike the case with the low salt buffer (20 mM BPES) (*38*) where no significant fluorescence quenching was observed.

DISCUSSION

Results obtained previously (*35*−*38*) have indicated that ADG is a good DNA intercalator exhibiting specificity toward alternating GC sequences. The present studies provide insight into the ability of this DNA intercalator to effectively stabilize DNA triple helical structures. A number of conclusions can be drawn from our present results that compare under identical conditions the interaction of ADG with triplexes and their duplex counterparts.

Binding of ADG to Duplex and Triplex DNA. The results presented here show that ADG has stronger binding toward DNA triplexes than to DNA duplexes. Primary evidence for this was the melting data where ADG stabilizes both the triplexes of T·A×T and C·G×C^+ sequences. A ΔT_m of ∼7 °C was observed with the T·A×T triplex against ∼3.5 °C with the C·G×C^+ triplex (Table 1), despite the 3-fold higher concentration of [Na^+] ions employed in the T·A×T experiments, but affinity is higher for C·G×C^+ than for T·A×T. Again, the T_m of the duplex was not affected in either case, indicating a preferential binding of ADG to the third strand of the triplexes. The higher degree of stabilization in the T·A×T−ADG complex in comparison to the C·G×C^+−ADG complex probably reflects differences in the molecular orientation at the interaction site and also the temperature at which the complex is melted. CD spectral data on these two triple helical DNA structures also clearly show that the binding of ADG perturbs the CD spectra in both cases. The changes in the CD spectra are more pronounced in the triplexes when compared with the respective duplexes. For the A·T duplex, under the experimental conditions described here, the effect of ADG binding was distinctly different from that observed earlier (*38*). At low ionic strength (20 mM [Na^+]), the CD spectrum of the A·T duplex was totally unaffected by ADG (*38*) whereas at 310 mM [Na^+] concentration ADG distinctly perturbed the CD spectrum of the A·T duplex. It has been suggested that the A·T duplex exists in a nonstandard right-handed conformation in low ionic strength solutions (*52*). However, at 310 mM [Na^+] this duplex structure is in a more standard B-form structure which shows a strong affinity for ADG, suggesting that polynucleotide structure is a key factor in the binding.

DNA structure as well as the sequence are the two important criteria for any ligand binding. Although the G·C duplex assumes a B-form structure under the normal pH and ionic conditions (*38*, *53*), there are reports that this polymer can adopt an unusual, ostensibly A-form (*51*). This duplex exhibits a B → A conformational transition upon increasing the ionic strength within the limit of 0.1−4.0 M (*42*). As observed earlier (*38*), CD spectral changes for the G·C duplex−ADG interaction are mostly confined to the negative CD band which gradually enhanced in the presence of the alkaloid. On the other hand, ADG effects changes to a varying extent on all the native CD bands of the corresponding triplex. In the 300−450 nm wavelength region, the shape and the magnitude of the extrinsic CD spectrum is significantly different and larger from that which was observed upon binding to the duplex structure. The likely explanation of this result is that the geometries of the bound molecule and its environment are not identical in the duplex and the triplex. The presence of a third strand in the major groove of the duplex has induced modifications that certainly favor binding of ADG to the triplex structure. If it is assumed that at 110 mM [Na^+] the G·C duplex is on the verge of a B → A conformational transition and the triple helical counterpart retains the characteristics of B-conformation in these solution conditions, the above difference in the CD spectral characteristics would indicate a stronger affinity of ADG to the triplex structure.

In spectrophotometric titration, the two DNA triplexes induced remarkable hypochromic and bathochromic effects on the absorption bands of ADG, with concomitant appearance of a single isosbestic point. These effects are particularly characteristic of an intercalative mode of binding to triplexes as suggested by Kim et al. (*19*). Such spectral changes were grossly similar to that observed with the corresponding duplexes, but significantly differed in several aspects, particularly in the T·A×T triplex case. For example, at low ionic strength (~20 mM [Na^+]) ADG does not bind to the A·T duplex, while at 310 mM of [Na^+] where the triplex is stable, ADG binds to the same duplex, exhibiting hypochromic and bathochromic effects. The binding parameters of ADG to triplex DNAs (Table 3) further advance evidence for a higher affinity of the alkaloid to these DNA triplexes in comparison to the respective duplexes. Especially noteworthy is the 5-fold increment in the binding constant of ADG with the T·A×T triplex. Again, in the case of the C·G×C^+ triplex, the K′ value reflects higher affinity of the alkaloid in comparison to its duplex. This higher binding affinity is further evident from the steady-state fluorescence studies where the binding to the C·G×C^+ triplex, rather than to the T·A×T triplex, remarkably quenches the intrinsic fluorescence intensity and decreases the fluorescence quantum yield. This study further shows that ADG binds more tightly to the triplex than to the duplex and that it selectively stabilizes the triple helix. Thus, it is apparent that on binding the alkaloid is located in a hydrophobic environment in the triplex as well as in the double helix. This kind of effect, especially for intercalators resting in hydrophobic environment after binding to a nucleic acid triple helix, was first demonstrated by Scaria and Shafer (*17*) and Mergny et al. (*18*).

A wide variety of DNA intercalators and minor groove binders have been shown to stabilize double helical structures, but fewer compounds have been found to interact with triple helical structures. Duplex intercalating ligands that have been shown to preferentially stabilize triplexes include ethidium, acridines, anthroquinones, benzo[*e*]pyridoindole, naphthoquinolines, and coralyne. Acridines, when covalently linked to the 5′ end of the third strand, have also been shown to stabilize the triplexes by intercalating at the duplex−triplex junction (*54*). Wilson and co-workers (*23*) reported that certain unfused aromatic quinolinium cations significantly increase melting temperature of the T·A×T triplex while having a much smaller effect on the melting temperature of the corresponding duplex. Helene and co-workers (*10, 55, 56*) described a series of benzopyridoindole derivatives that stabilize both T·A×T and C·G×C^+ triplexes more than they do to the corresponding duplexes. Recently, several anthraquinone sulfonamide derivatives have been found to stabilize the T·A×T triplex without significantly affecting the corresponding duplex (*46*). Scaria and Shafer (*17*) studied the comparative binding aspects of ethidium intercalation to the A·T duplex and T·A×T triplex and showed that binding is stronger to the triplex than to the duplex. On the contrary, Mergny et al. (*18*), using a 22-mer oligonucleotide triplex having 15 T·A×T and 7 C·G×C^+ triplexes, showed that ethidium binds more weakly to the triplex than to the corresponding duplex. Some minor groove binding ligands interact with triple helices but destabilize them (*57*) except for berenil which is reported to stabilize the DNA triplex in the absence of NaCl (*41*). Benzopyriodoindoles were shown (*10*) to bind to a triplex more tightly than to a duplex. It was reported that coralyne could also stabilize T·A×T and C·G×C^+ containing intra- and intermolecular triple helices (*20*), but it has greater affinity toward the T·A×T triplex (*21*). It can be assumed that the stacking arrangement between the intercalator and the third strand may play an important role in the triplex stability as the template duplex is not found to be significantly stabilized by an intercalator. In the case of ADG, the transient positive charge formation in the N6 position during its interaction with nucleic acids, as demonstrated by Chakraborty et al. (*36*), may cause a relief of electrostatic repulsions among the negatively charged phosphate backbone of the three DNA strands. This may, in turn, work as a positive and important contribution toward triplex stabilization as shown in several other cases also (*22, 46, 54*). In this regard it is worth noting that all intercalative triplex binding ligands described to date possess a cationic chromophore and selectively stabilize the T·A×T rather than the C·G×C^+ triplex. The only exception to this is coralyne where both T·A×T and C·G×C^+ triplexes are stabilized. ADG stabilizes the C·G×C^+ triplexes, and the affinity is observed to be very high. It is most likely that the transient charge in ADG is released on binding leading to a favorable orientation at the intercalation site in the C·G×C^+ triplex, thereby the protonated cytosine is not disfavoring the stability of the complex.

Binding of ADG to Duplex and Triplex RNA. The alkaloid ADG has been shown to interact with triplex and duplex RNA by various spectroscopic measurements under identical experimental conditions. Thermal melting profiles indicate that binding of ADG to the triple helix U·A×U resulted in a lowering of the melting temperature of the third strand from the triplex, but the duplex template thereafter melts at a higher temperature. In this regard, the behavior of ADG is similar to that of ethidium which stabilizes the RNA duplex and destabilizes the triplex structure (*29*). This result is further supported by the CD study. Binding to either form induces perturbation to CD bands, but changes are more pronounced in the triplex. The presence of the extrinsic CD bands in the 300−450 nm region for the complexes of ADG with duplex and triplex RNA shows that the bound ADG is in an asymmetric environment. The amplitude of the extrinsic CD band is remarkably higher in the triplex than in the duplex. Such differences would also arise from the nature of the binding site and/or differences in base orientation in the two complexes apart from the propensity of the bound molecules. In the case of the U·A×U triplex, a higher binding affinity (Table 3) to the triplex compared to that of the A·U duplex was observed. In contrast, the UV melting results (Figure 3C) show that the ligand destabilizes the triplex in that it lowers the first melting transition ascribed to dissociation of the third strand from the triplex. This can be interpreted in terms of the different orientation of the ADG molecule at the binding site in the duplex and triplex strcture of RNA, as the glucoside ring in ADG being noncoplanar with the rest of the molecule (*34*) produces a significant effect in thermal destabilization.

Although we cannot specify the exact binding geometry of the ADG−triplex complex, we can deduce some key features of the binding model in light of the experimental observations. The strong hypochromic and bathochromic

effects observed on binding of ADG to triplexes lead us to suggest an intercalative environment for the bound ADG molecules inside the Hoogsteen base-paired third strand, facilitating the effective electronic coupling required for stabilizing the third strand. Further, CD spectral data, particularly the extrinsic CD, also indicate an effective coupling between the electronic transitions of ADG and base pairs in triplex. The quenching of the steady-state fluorescence also substantiates the argument that ADG is buried in the stack of Hoogsteen base pairs of the third strand. Taken together, these features strongly point to an intercalation geometry for ADG in the triplexes. Further investigations with model systems involving small oligonuclotides are required to conclusively prove the molecular details of the ADG−triplex association.

CONCLUSIONS

The present study shows that the naturally occurring alkaloid, ADG, preferentially stabilizes the triplex structures of DNA in comparison to their duplex structures, presumably by intercalating between the Hoogsteen base-paired third strand in the major groove. The GC sequence specificity exhibited in the duplex binding is again exhibited in triplex binding as shown by a higher binding affinity to the C·G×C$^+$ triplex in comparison to the T·A×T triplex. ADG also exhibits a higher affinity for the RNA triplex in comparison to the RNA duplex, but causes the Hoogsteen base-paired third strand to dissociate at a lower temperature.

ACKNOWLEDGMENT

A. Ray and S. Das are indebted to the University Grants Commission, Government of India, for the award of Senior and Junior Research Fellowships.

SUPPORTING INFORMATION AVAILABLE

Three figures showing CD spectral changes, fluorescence spectral changes, and fluorescence quantum yield data of ADG−duplex and ADG−triplex complexes. This information is available free of charge via the Internet at http://pubs.acs.org.

REFERENCES

1. Felsenfeld, G., Davies, D. R., and Rich, A. (1957) *J. Am. Chem. Soc. 79*, 2023−2024.
2. Thoung, N. T., and Helene, C. (1993) *Angew. Chem., Int. Ed. Engl. 32*, 666−690.
3. Moser, H. E., and Dervan, P. B. (1987) *Science 238*, 645−650.
4. Rajagopal, P., and Feigon, J. (1989) *Nature 339*, 637−640.
5. Pilch, D. S., Levenson, C., and Shafer, R. H. (1991) *Biochemistry 30*, 6081−6087.
6. Sun, J.-S., and Helene, C. (1993) *Curr. Opin. Struct. Biol. 3*, 345−356.
7. Gowers, D. M., and Fox, K. R. (1997) *Nucleic Acids Res. 25*, 3787−3794.
8. Chastain, M., and Tinoco, I., Jr. (1992) *Nucleic Acids Res. 20*, 315−318.
9. Frank-Kamenetskii, M. D., and Mirkin, S. M. (1995) *Annu. Rev. Biochem. 64*, 65−95.
10. Escude, C., Nguyen, C. H., Mergny, J.-L., Sun, J.-S., Bisagni, E., Garestier, T., and Helene, C. (1995) *J. Am. Chem. Soc. 117*, 10212−10219.
11. Sun, J.-S., Garestier, T., and Helene, C. (1996) *Curr. Opin. Struct. Biol. 6*, 327−333.
12. Choi, S.-D., Kim, M.-S., Kim, S. K., Lincoln, P., Tuite, E., and Norden, B. (1997) *Biochemistry 36*, 214−223.
13. Musso, M., Thomas, T., Shirahata, A., Sigal, L. H., van Dyke, M. W., and Thomas, T. J. (1997) *Biochemistry 36*, 1441−1449.
14. Shindo, H., Matsumoto, N., and Shimzu, M. (1997) *Nucleic Acids Res. 25*, 4786−4791.
15. Quali, M., Gousset, H., Geinguenand, F., Liquier, J., Gabarro, A., Bret, M. L., and Taillandier, E. (1997) *Nucleic Acids Res. 25*, 4816−4824.
16. Srinivasan, A. R., and Olson, W. K. (1998) *J. Am. Chem. Soc. 120*, 484−491.
17. Scaria, P. V., and Shafer, R. H. (1991) *J. Biol. Chem. 266*, 5417−5423.
18. Mergny, J. L., Collier, D., Rougee, M., Montenary-Garestier, T., and Helene, C. (1991) *Nucleic Acids Res. 19*, 1521−1526.
19. Kim, H.-K., Kim, J.-M, Kim, S. K., Rodger, A., and Norden, B. (1996) *Biochemistry 35*, 1187−1194.
20. Lee, J. S., Latimer, L. J. P., and Hampel, K. J. (1993) *Biochemistry 32*, 5591−5597.
21. Moraru-Allen, A. A., Cassidy, S., Alvarez, J. L. A., Fox, K. R., Brown, T., and Lane, A. N. (1997) *Nucleic Acids Res. 25*, 1890−1896.
22. Fox, K. R., Polucci, P., Jenkins, T. C., and Neidle, S. (1995) *Proc. Natl. Acad. Sci. U.S.A. 92*, 7887−7891.
23. Wilson, W. D., Tanious, F. A., Mizan, S., Yao, S., Kiselyov, A. S., Zon, G., and Strekowski, L. (1993) *Biochemistry 32*, 10614−10621.
24. Chandler, S. P., Strekowski, L., Wilson, W. D., and Fox, K. R. (1995) *Biochemistry 34*, 7234−7242.
25. Merchand, C., Bailly, C., Nguyen, C. H., Bisagni, E., Garestier, T., Helene, C., and Waring, M. J. (1996) *Biochemistry 35*, 5022−5032.
26. Roberts, R. W., and Crothers, D. M. (1992) *Science 258*, 1463−1466.
27. Han, H., and Dervan, P. B. (1993) *Proc. Natl. Acad. Sci. U.S.A. 90*, 3806−3810.
28. Liquier, J., Taillandier, E., Klinck, R., Guittet, E., Gouyette, C., and Huynh-Dinh, T. (1995) *Nucleic Acids Res. 23*, 1722−1728.
29. Waring, M. J. (1974) *Biochem. J. 143*, 483−486.
30. Lehrman, E. A., and Crothers, D. M. (1977) *Nucleic Acids Res. 4*, 1381−1392.
31. Pilch, D. S., and Breslauer, K. J. (1994) *Proc. Natl. Acad. Sci. U.S.A. 91*, 9332−9336.
32. Chen, Z., and Zhu, D. (1987) in *The Alkaloids* (Brossi, A., Ed.) Vol. 31, pp 29−65, Academic Press, Orlando, Fl.
33. Cassady, J. M., Baird, W. B., and Cheng, C. (1990) *J. Nat. Prod. Lloydia 53*, 23−41.
34. Chakraborty, S., Nandi, R., Maiti, M., Achari, B., and Bandyopadhyay, S. (1989) *Photochem. Photobiol. 50*, 685−689.
35. Chakraborty, S., Nandi, R., Maiti, M., Achari, B., Saha, C. R., and Pakrashi, S. C. (1989) *Biochem. Pharmacol. 38*, 3683−3687.
36. Chakraborty, S., Nandi, R., and Maiti, M. (1990) *Biochem. Pharmacol. 39*, 1181−1186.
37. Maiti, M. (1991) *Indian J. Phys. 65B*, 385−397.
38. Nandi, R., Chakraborty, S., and Maiti, M. (1991) *Biochemistry 30*, 3715−3720.
39. Ray, A., and Maiti, M. (1996) *Biochemistry 35*, 7394−7402.
40. Sen, A., Ray, A., and Maiti, M. (1996) *Biophys. Chem. 59*, 155−170.
41. Pilch, D. S., Kirolos, M. A., and Breslauer, K. J. (1995) *Biochemistry 34*, 16107−16124.
42. Quali, M., Letellier, R., Adnet, F., Liquier, J., Sun, J.-S., Lavery, R., and Taillandier, E. (1993) *Biochemistry 32*, 2098−2103.
43. Buckin, V., Tran, H., Morozov, V., and Marky, L. A. (1996) *J. Am. Chem. Soc. 118*, 7033−7039.
44. Tuite, E., and Norden, B. (1995) *Bioorg. Med. Chem. 3*, 701−711.

45. Johnson, K. H., Gray, D. M., and Sutherland, J. C. (1991) *Nucleic Acids Res. 19*, 2275−2280.
46. Kan, Y., Armitage, B., and Schuster, G. B. (1997) *Biochemistry 36*, 1461−1466.
47. Crothers, D. M. (1968) *Biopolymers 6*, 575−584.
48. McGhee, J. D., and von Hippel, P. H. (1974) *J. Mol. Biol. 86*, 469−489.
49. Ray, A., Maiti, M., and Nandy, A. (1996) *Comput. Biol. Med. 26*, 497−503.
50. Nandy, A., Kumar, G. S., and Maiti, M. (1993) *Indian J. Biochem. Biophys. 30*, 204−208.
51. Tuite, E., Lincoln, P., and Norden, B. (1997) *J. Am. Chem. Soc. 119*, 239−240.
52. Herrera, E. J., and Chaires, B. J. (1989) *Biochemistry 28*, 1993−2000.
53. Mercado, C. M., and Tomasz, M. (1977) *Biochemistry 16*, 2040−2046.
54. Cassidy, S. A., Strekowski, L., Wilson, W. D., and Fox, K. R. (1994) *Biochemistry 33*, 5338−5347.
55. Mergny, J. L., Duval-Valentin, G., Nguyen, C. H., Perroualt, L., Faucon, B., Rougee, M., Montenary-Garestier, T., Bisagni, E., and Helene, C. (1992) *Science 256*, 1681−1684.
56. Silver, G. C., Sun, J-.S., Nguyen, C. H., Boutorine, A. S., Bisagni, E., and Helene, C. (1997) *J. Am. Chem. Soc. 119*, 263−268.
57. Durand, M., Thuong, N. T., and Maurizot, J. C. (1992) *J. Biol. Chem. 267*, 24394−24399.

BI982128N